Research Square

Preprints are preliminary reports that have not undergone peer review.
They should not be considered conclusive, used to inform clinical practice,
or referenced by the media as validated information.

Sensor Fault Detection in Networked Control Systems Under Disturbances and Communication Imperfections

Reda El Abbadi

r.elabbadi@uiz.ac.ma

LAMISNE, Ibn Zohr University

Khalid Badie

Cadi Ayyad University

Laila Dami

Cadi Ayyad University

Samir Elouaham

National School of Applied Sciences, Ibn Zohr University

Mohamed Louzazni

National School of Applied Sciences, Chouaib Doukkali University of El Jadida

Research Article

Keywords:

Posted Date: September 16th, 2025

DOI: https://doi.org/10.21203/rs.3.rs-7277315/v1

License: This work is licensed under a Creative Commons Attribution 4.0 International License.
Read Full License

Additional Declarations: No competing interests reported.

Sensor Fault Detection in Networked Control Systems Under Disturbances and Communication Imperfections

Reda El Abbadi[a,*], Khalid Badie[b], Laila Dami[b], Samir Elouaham[c], Mohamed Louzazni[d]

[a]*LAMISNE, Polydisciplinary Faculty of Taroudant, Ibn Zohr University, Agadir, Morocco.*
[b]*Mathematics, Modeling and Automatic Systems Laboratory, Faculty of Science Semlalia, Cadi Ayyad University, Marrakesh, Morocco;*
[c]*Laboratory of Systems Engineering and Information Technology (LISTI), National School of Applied Sciences, Ibn Zohr University, Agadir, Morocco.*
[d]*Science Engineer Laboratory for Energy, National School of Applied Sciences, Chouaib Doukkali University of El Jadida, El Jadida, Morocco.*

Abstract

This paper addresses the problem of sensor fault detection in Networked Control Systems (NCS) subject to communication imperfections, including time-varying delays and packet dropouts. These network-induced constraints can significantly degrade system performance and hinder timely fault identification. To model the stochastic behaviour of the communication network, Markov chains are used to represent the random nature of delays and packet losses. A fault detection strategy is proposed based on a Lyapunov function framework and Linear Matrix Inequality (LMI) techniques. The approach establishes sufficient conditions for fault detectability formulated as LMIs, ensuring robustness against the probabilistic uncertainties of the network. Simulation results confirm the effectiveness and reliability of the proposed method in detecting sensor faults under varying network conditions.

1. Introduction

In recent years, Networked Control Systems (NCSs) have gained significant attention due to their flexibility, scalability, and cost-effectiveness [1]. In such systems, control loops are closed through a communication network, allowing sensors, controllers, and actuators to be spatially distributed and interconnected [2]. Among these components, sensors play a critical role, as they are responsible for acquiring real-time data from the physical environment and transmitting it to the controller for decision-making [3].

Unlike traditional control systems where sensors are directly wired to the controller, sensors in NCSs operate over shared communication channels, such as wireless or Ethernet networks. This networked configuration offers several advantages, including easier system reconfiguration, remote monitoring, and reduced wiring complexity [1]. This installation

*Corresponding author
Email address: r.elabbadi@uiz.ac.ma (Reda El Abbadi)

is widely used in modern applications such as industrial automation [4], autonomous vehicles [5], smart cities [6, 7], smart agriculture [8], and healthcare monitoring systems [9]. However, this architecture also introduces several challenges, including packet dropouts, time-varying delays, limited bandwidth, and potential cyber-security vulnerabilities [10].

While NCS offer flexibility and scalability, they are also susceptible to network-induced issues such as packet dropouts and communication delays [11], which can degrade system performance or even lead to instability. Under such constraints, the occurrence of sensor faults becomes more difficult to detect and isolate, as it may be confused with network problems or masked by data loss. Therefore, early detection and diagnosis of sensor faults is crucial to ensure the reliability and safety of NCS. Faults left undetected can propagate through the system, leading to incorrect control actions or system failures [12]. The challenge is exacerbated in environments with unreliable communication, where distinguishing between a faulty sensor and a delayed or missing data packet becomes a complex task. Developing robust fault detection methods that can operate effectively in the presence of packet loss and network delay is thus a vital research area for enhancing the resilience of intelligent control systems. In the literature, several studies have addressed the problem of sensor fault detection in NCS. For example, Shi-Yuan Han et al in [13] addressed the problem of sensor faults and delay-tolerant control in NCSs affected by external disturbances. They reformulated the original control problem into an equivalent one by redefining the available system output and modifying the performance index. To tackle the issue, a Feedforward and Feedback Sensor Fault-Tolerant Controller (FFSFTC) was developed using the solutions of the Riccati and Stein matrix equations. Additionally, a fault diagnoser was designed, allowing the controller to be restructured in a way that compensates for both sensor faults and the effects of delayed measurements. Another relevant study is that of Yu-Yan Zhang et al [14], where the authors considered the presence of packet dropouts in the communication network. In their work, a fault model was developed based on potential sensor and actuator faults, and Model Predictive Control (MPC) was employed to compensate for communication delays. When the sensors and actuators operate normally, an H_∞ stability criterion for the state predictive observer is formulated using Linear Matrix Inequality (LMI) techniques.

In this paper, a fault detection approach is developed to identify sensor faults despite the presence of communication limitations such as packet dropouts and communication delays. The approach begins by defining an accurate mathematical model of the system that accounts for all network-related issues. A Markov chain is used to represent the stochastic behaviour of these communication problems. To formulate the fault detection problem, a Lyapunov function is employed, which leads to a Linear Matrix Inequality (LMI) representation. This LMI incorporates all relevant system information, including the system model and the probability of network-induced events. To enhance realism, sensor noise is introduced into the model. Inspired by the work of Benzaouia et al. [15], slack variables are added to the LMI to increase its flexibility, thereby improving the chances of finding feasible solutions for the controller and observer gains.

2. System Description and Network Architecture

In an NCS, sensors, controllers, and actuators are spatially distributed across different physical locations and communicate over a shared network **Figure** 1. This spatial distribution enables flexible and scalable system architectures, where sensing, computation, and actuation can occur at different points in the system. Sensors are typically deployed close to the physical processes they monitor, while controllers may be located centrally or remotely to process data and make decisions. Actuators are positioned near the components they influence, executing control commands received through the network. While this distributed setup offers numerous advantages such as easier maintenance, modularity, and cost reduction, it also introduces challenges related to communication delays, packet losses, and synchronization, which can affect the overall system performance and stability.

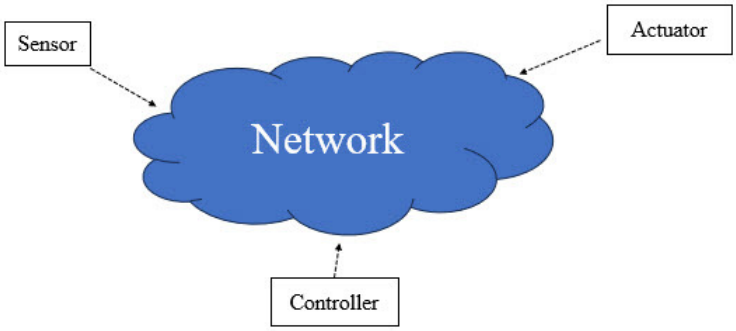


Figure 1: Network Architecture

In the literature, various approaches have been proposed to model NCS. However, the majority of studies adopt two primary modelling strategies, depending on the placement of the wireless communication network within the system architecture. Specifically, the wireless network can be located between the sensor and controller (S–C) [16, 17], between the controller and actuator (C–A), or in both segments [10, 18]. The wireless network introduces two main constraints: packet loss and network-induced delays. Numerous mathematical models have been developed to characterize these phenomena. Packet loss is often modelled using probabilistic frameworks, with many studies representing it as a binary switching sequence governed by a Bernoulli process [19]. In contrast, network-induced delays can be modelled as constant, time-varying, or stochastic processes, with Markov chains frequently used to capture their probabilistic behaviour [18].

In this study, packet loss is assumed to occur simultaneously in both S-C and C-A communication links. Additionally, the effect of network-induced delays is taken into account, as illustrated in **Figure 2**. The wireless communication network is modelled using switches S_i, where $i = 1, 2$, representing the S-C and C-A channels, respectively. Each switch operates arbitrarily, with a closed state indicating a successful packet transmission and an open state signifying a packet dropout. The switching behaviour of S_1 and S_2 can

be described by the following dynamic model:

$$\begin{cases} \bar{y}(k) = \alpha(k)\ y(k - \tau_1(k)), \\ \bar{u}(k) = \beta(k)\ u(k - \tau_2(k)). \end{cases} \tag{1}$$

where,

$$\alpha(k), \beta(k) = \begin{cases} 0 \text{ if the packet is lost,} \\ 1 \text{ if the packet is received.} \end{cases} \tag{2}$$

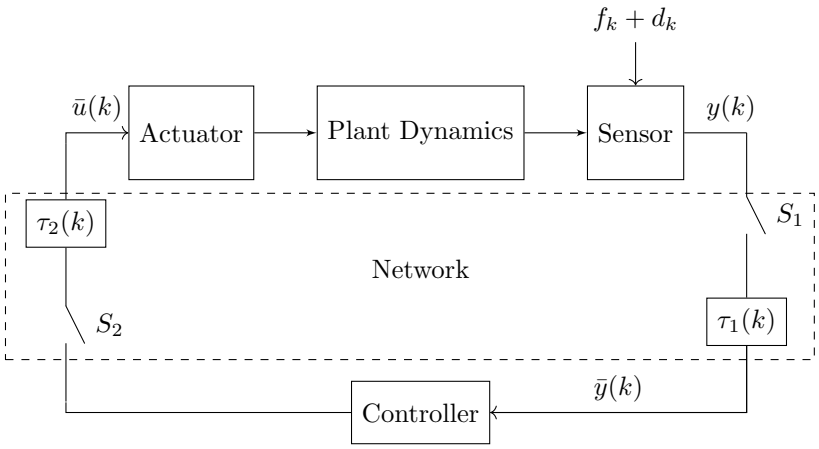


Figure 2: Network architecture.

The states of switches S_1 and S_2 are determined by the binary variables $\alpha(k)$ and $\beta(k)$. The Markov chain $\mu(k)$ is used to represent the combined state of both switches. It can take one of four discrete values, each corresponding to a unique combination of α and β, as described below:

- When $\alpha = 0$ and $\beta = 0$ (i.e., $\mu(k) = 1$), both switches S_1 and S_2 are open.
- When $\alpha = 0$ and $\beta = 1$ (i.e., $\mu(k) = 2$), switch S_1 is open and switch S_2 is closed.
- When $\alpha = 1$ and $\beta = 0$ (i.e., $\mu(k) = 3$), switch S_1 is closed and switch S_2 is open.
- When $\alpha = 1$ and $\beta = 1$ (i.e., $\mu(k) = 4$), both switches S_1 and S_2 are closed.

The random time delays $\tau_i(k)$ occurring in S-C and C-A channels are assumed to be bounded within two positive limits, meaning that $0 \leq \tau_i^{\min} \leq \tau_i(k) \leq \tau_i^{\max}$ for $i = 1, 2$.

In this work, the communication delays $\tau_1(k)$ and $\tau_2(k)$ are represented as two homogeneous Markov chains, each taking values from a finite set: $\mathcal{L}_1 = [0, 1, \ldots, \tau_1^{\max}]$ and $\mathcal{L}_2 = [0, 1, \ldots, \tau_2^{\max}]$. Accordingly, the transition probabilities are given by:

$$\begin{cases} \mathbb{P}\{\mu(k+1) = j | \mu(k) = i\} = \Pi_{ij}, \\ \mathbb{P}\{\tau_1(k+1) = n | \tau_1(k) = m\} = \Psi_{mn}, \\ \mathbb{P}\{\tau_2(k+1) = q | \tau_2(k) = p\} = \Omega_{pq}, \end{cases} \tag{3}$$

where $\Pi_{ij} \geq 0$, $\Psi_{mn} \geq 0$, and $\Omega_{pq} \geq 0$ for all $i, j \in [1, ..., 4]$, $m, n \in \mathcal{L}_1$, $p, q \in \mathcal{L}_2$ and

$$\sum_{j=1}^{4} \Pi_{ij} = 1, \sum_{n=0}^{\tau_1^{max}} \Psi_{mn} = 1, \sum_{q=0}^{\tau_2^{max}} \Omega_{pq} = 1. \tag{4}$$

3. System Modelling

Consider a discrete-time NCS subject to a sensor fault and an external disturbance, as illustrated in **Figure 2**. The state space of the global system can be written as follows:

$$\begin{cases} x(k+1) & = Ax(k) + B\bar{u}(k), \\ y(k) & = Cx(k) + Ff(k) + Ed(k), \end{cases} \tag{5}$$

where $x(k) \in \mathbb{R}^n$ is the state vector, the vector $\bar{u}(k) \in \mathbb{R}^m$ is the control input, the vectors $y(k)$ and $\bar{y}(k) \in \mathbb{R}^p$ are the measured output and the converted output, respectively. $f(k) \in \mathbb{R}^m$ is the sensor fault vector. $d(k) \in \mathbb{R}^w$ is an external disturbance. $A \in \mathbb{R}^{n \times n}$, $B \in \mathbb{R}^{n \times m}$, $C \in \mathbb{R}^{p \times n}$, $F \in \mathbb{R}^{n \times m}$, and $E \in \mathbb{R}^{n \times 1}$ are the system matrices.

The developed fault detection filter is given as follows:

$$\begin{cases} \hat{x}(k+1) & = A\hat{x}(k) + Bu(k) + L(\bar{y}(k) - \alpha(k)\hat{y}(k - \tau_1(k))), \\ \hat{y}(k) & = C\hat{x}(k), \\ r(k) & = V(\bar{y}(k) - \alpha(k)\hat{y}(k - \tau_1(k))), \end{cases} \tag{6}$$

where $\hat{x}(k) \in \mathbb{R}^n$ is the filter state vector, $\hat{y}(k) \in \mathbb{R}^p$ is the output vector of the filter, L is the filter gain matrix, $r(k) \in \mathbb{R}^m$ is the residual vector, and V is the residual gain matrix. The feedback control law is given as follows:

$$u(k) = K\hat{x}(k), \tag{7}$$

where K represents the state feedback gain matrix. The state estimation error is defined as follows:

$$e(k) = x(k) - \hat{x}(k). \tag{8}$$

From the above equations, we can obtain the closed-loop system as:

$$\begin{cases} \phi(k+1) = \mathcal{A}\phi(k) + \mathcal{B}_1(\mu(k))\phi(k - \tau_1(k)) + \mathcal{B}_2(\mu(k))\phi(k - \tau_2(k)) + \mathcal{B}_3 w(k - \tau_1(k))), \\ \phi(k) = \nu(k), k \in \{-max(\tau_1, \tau_2), ..., 0\}, \end{cases} \tag{9}$$

where,

$$\mathcal{A} = \begin{bmatrix} A & 0 \\ -BK & A + BK \end{bmatrix}, \mathcal{B}_1 = \alpha_k \begin{bmatrix} 0 & 0 \\ 0 & -LC \end{bmatrix}, \mathcal{B}_2 = \beta_k \begin{bmatrix} BK & -BK \\ BK & -BK \end{bmatrix}, \mathcal{B}_3 = \alpha_k \begin{bmatrix} 0 & 0 \\ -LF & -LE \end{bmatrix},$$

and the augmented vectors are defined as:

$\phi(k) = [x^T(k) \;\; e^T(k)]^T$, $w(k-\tau_1(k)) = [d^T(k-\tau_1(k)) \;\; f^T(k-\tau_1(k))]^T$.

The aim of this article is to find the filter gain and the controller gain matrices for the system such that, when $w = 0$, system (9) is stochastically stable, and under system zero initial conditions, the residual error r_k satisfies the following H_∞ performance:

$$\mathbb{E}\left\{ \sum_{k=0}^{N-1} r_k^T r_k \right\} \leq \gamma^2 \mathbb{E}\left\{ \sum_{k=0}^{N-1} w_{k-\tau_1}^T w_{k-\tau_1} \right\} \tag{10}$$

Remark

The summation in (10) includes the delayed signal $w_{k-\tau_1}$. If $k - \tau_1 < 0$ (i.e., the delay refers to a time before the system starts), then $w_{k-\tau_1} = 0$ for $k < \tau_1$.

4. Residual Function and Threshold

The evaluation of the residual function and the threshold J_{th} are defined as:

$$J_k = \mathbb{E}\left\{ \sum_{\rho=k_0}^{k_0+k} \sqrt{r^T(\rho) r(\rho)} \right\}, \tag{11}$$

$$J_{th} = \sup_{w_k \in L_2, f_k = 0} \mathbb{E}\left\{ \sum_{\rho=k_0}^{k_0+k} \sqrt{r^T(\rho) r(\rho)} \right\}, \tag{12}$$

where k_0 denotes the initial evaluation time instant. The window size will increase continuously until it is equal to the limited size of the global observation horizon. Then, J_k will be compared to J_{th} to identify if a fault appears or not.

$$\begin{aligned} &J_k > J_{th} \Rightarrow \text{Alarm for fault,} \\ &J_k \leq J_{th} \Rightarrow \text{No fault.} \end{aligned} \tag{13}$$

The condition (10) is realized if:

$$J(\gamma) = \mathbb{E}\left\{ \sum_{k=0}^{N-1} [r_k^T r_k - \gamma^2 w_{k-\tau_1}^T w_{k-\tau_1}] \right\} \leq 0, w_{k-\tau_1} = 0 \quad for \quad k < \tau_1. \tag{14}$$

In order to realize the condition (14), a Lyapunov function is used to find the following condition:

$$\mathbb{E}\left\{ \sum_{k=0}^{N-1} [r_k^T r_k - \gamma^2 w_{k-\tau_1}^T w_{k-\tau_1} + \Delta V_k] \right\} < 0. \tag{15}$$

where,

$$r_k^T r_k = \phi_{k-\tau_{1(k)}}^T \mathcal{D}_1^i \phi_{k-\tau_{1(k)}} + \phi_{k-\tau_{1(k)}}^T \mathcal{D}_2^i w_{k-\tau_{1(k)}} + w_{k-\tau_{1(k)}}^T \mathcal{D}_3^i w_{k-\tau_{1(k)}} \tag{16}$$

and,

$$\mathcal{D}_1^i = \alpha_k^2 \begin{bmatrix} 0 & 0 \\ 0 & C^T V^T V C \end{bmatrix}, \mathcal{D}_2^i = \alpha_k^2 \begin{bmatrix} 0 & 0 \\ C^T V^T V F & C^T V^T V E \end{bmatrix}, \mathcal{D}_3^i = \alpha_k^2 \begin{bmatrix} F^T V^T V F & F^T V^T V E \\ * & E^T V^T V E \end{bmatrix}$$

5. Supporting Lemmas

Lemma 5.1 (Schur Complement)**.** *[20] Let $A = A^\top \in \mathbb{R}^{n\times n}$, $B \in \mathbb{R}^{n\times m}$, and $C = C^\top \in \mathbb{R}^{m\times m}$. Then the following statements are equivalent:*

1. $$\begin{bmatrix} A & B \\ B^\top & C \end{bmatrix} \prec 0$$
2. $C \prec 0$ *and* $A - BC^{-1}B^\top \prec 0$

provided that C is invertible.

Lemma 5.2. *[15] If $\mathcal{P}^{-1} > 0$, the following development:*

$$(G^T - \mathcal{P})\mathcal{P}^{-1}(G - \mathcal{P}) = G^T\mathcal{P}^{-1}G - G^T - G + \mathcal{P} > 0. \tag{17}$$

Leads to,

$$-G^T\mathcal{P}^{-1}G < -G^T - G + \mathcal{P}. \tag{18}$$

Lemma 5.3. *[21] Given symmetric matrix $\mathcal{C}$ and matrices $\mathcal{L}$, $\Phi(k)$ and $\mathcal{H}$ with appropriate dimension.*

$$\mathcal{C} + \mathcal{L}^T\Phi(k)\mathcal{H} + \mathcal{H}^T\Phi^T(k)\mathcal{L} < 0, \tag{19}$$

holds for $\Phi^T(k)\Phi(k) \leq I$ if only if there exists a positive scalar ϵ such that:

$$\mathcal{C} + \epsilon^{-1}\mathcal{L}^T\mathcal{L} + \epsilon\mathcal{H}^T\mathcal{H} < 0. \tag{20}$$

6. Main Results

In this section, a stochastic Lyapunov-Krasovskii functional is constructed and utilized as a key tool to analyse the stability and detect sensor faults in an NCS with communication network imperfections. Based on this functional, sufficient conditions for the asymptotic stability of the system (9) are formulated in terms of LMIs. By solving the derived LMIs using convex optimization techniques, one can simultaneously compute the gain matrices K of the state-feedback controller and the fault detection filter L. These gains ensure that the system maintains desired performance and stability while effectively detecting sensor faults under the constraints imposed by the networked environment.

Theorem 6.1. *Given positive scalars γ, ϵ_1, ϵ_2, ϖ_1, and ϖ_2, the system (9) is said to be asymptotically stable if there exist matrices $P_{i,m,p} > 0$ for all $i \in [1, 4]$, $m \in \mathcal{L}_1$, and*

$p \in \mathcal{L}_2$, *along with positive definite matrices* Q_1, Q_2, Q_3, Q_4, X_1, *and* X_2, *and matrices* K *and* L *of suitable dimensions, such that the following conditions are satisfied:*

$$\begin{bmatrix} \hat{\psi}_{11} & \hat{\psi}_{12} & \hat{\psi}_{13} & 0 & \cdots & \cdots & \hat{\psi}_{17} & 0 & 0 & \mathcal{X}_1 & \mathcal{X}_2 \\ * & \psi_{22} & 0 & \cdots & 0 & 0 & 0 & \mathcal{B}_K & \vdots & \cdots & \cdots \\ * & * & \psi_{33} & \ddots & 0 & 0 & \psi_{37} & 0 & \vdots & \vdots & \vdots \\ * & * & * & \psi_{44} & \ddots & 0 & 0 & \vdots & -\mathcal{B}_K & \vdots & \vdots \\ * & * & * & * & \psi_{55} & \ddots & \vdots & \vdots & 0 & \vdots & \vdots \\ * & * & * & * & * & \psi_{66} & \ddots & \vdots & \vdots & \vdots & \vdots \\ * & * & * & * & * & * & \psi_{77} & \ddots & \vdots & \vdots & \vdots \\ * & * & * & * & * & * & * & -\epsilon_1^{-1} & \ddots & \vdots & \vdots \\ * & * & * & * & * & * & * & * & -\epsilon_2^{-1} & \ddots & \vdots \\ * & * & * & * & * & * & * & * & * & -\hat{\epsilon}_1 & \vdots \\ * & * & * & * & * & * & * & * & * & * & -\hat{\epsilon}_2 \end{bmatrix} < 0, \tag{21}$$

where,

$$\begin{aligned}
\hat{\psi}_{11} &= -G^T - G + \bar{P}_{i,m,p}, \\
\hat{\psi}_{12} &= G\bar{\mathcal{A}}, \\
\hat{\psi}_{13} &= G\mathcal{B}_1^i, \\
\hat{\psi}_{17} &= G\mathcal{B}_3, \\
\psi_{22} &= -P_{i,m,p} + Q_1 + Q_2 + (1+\tau_1)Q_3 + (1+\tau_2)Q_4, \\
\psi_{33} &= -Q_1 + \mathcal{D}_1, \\
\psi_{44} &= -Q_2, \\
\psi_{55} &= -Q_3, \\
\psi_{66} &= -Q_4, \\
\psi_{37} &= \mathcal{D}_2, \\
\psi_{77} &= \mathcal{D}_3 - \gamma^2 I, \\
G &= \begin{bmatrix} X_1 & 0 \\ 0 & X_2 \end{bmatrix}, \\
\bar{\mathcal{A}} &= diag(A, A), \\
\mathcal{B}_K &= [-BK \quad BK]^T, \\
\mathcal{X}_1 &= [\beta_k X_1 \quad \beta_k X_2]^T, \\
\mathcal{X}_2 &= [0 \quad X_2]^T, \\
\hat{\epsilon}_1 &= 2\varpi_1 I - \varpi_1^2 \epsilon_1^{-1}, \\
\hat{\epsilon}_2 &= 2\varpi_2 I - \varpi_2^2 \epsilon_2^{-1}.
\end{aligned}$$

proof. Consider the following Lyapunov-Krasovskii functional:

$$V(\phi_k, \mu_k, \tau_{1k}, \tau_{2k}) = V_1 + V_2 + V_3, \tag{22}$$

where,

$$V_1 = \phi_k^T P_{\mu_k,\tau_{1k},\tau_{2k}} \phi_k,$$
$$V_2 = \sum_{l=k-\tau_1}^{k-1} \phi_l^T Q_1 \phi_l + \sum_{l=k-\tau_2}^{k-1} \phi_l^T Q_2 \phi_l,$$
$$V_3 = \sum_{l=k-\tau_1(k)}^{k-1} \phi_l^T Q_3 \phi_l + \sum_{r=-\tau_1+1}^{0} \sum_{s=k+r}^{k-1} \phi_s^T Q_3 \phi_s + \sum_{l=k-\tau_2(k)}^{k-1} \phi_l^T Q_4 \phi_l + \sum_{r=-\tau_2+1}^{0} \sum_{s=k+r}^{k-1} \phi_s^T Q_4 \phi_s,$$

The mathematical expectation of the forward difference of the Lyapunov-Krasovskii functional is:

$$\mathbb{E}\{\Delta V(\phi_k, \mu_k, \tau_{1k}, \tau_{2k})\} = \mathbb{E}\{\Delta V_1\} + \mathbb{E}\{\Delta V_2\} + \mathbb{E}\{\Delta V_3\}, \tag{23}$$

where,

$$\begin{aligned}
\mathbb{E}\{\Delta V_1\} &= \mathbb{E}\{\phi_{k+1}^T P_{\mu_{k+1},\tau_{1(k+1)},\tau_{2(k+1)}} \phi_{k+1} \mid \mu_k = i, \tau_{1(k)} = m, \tau_{2(k)} = p\} - \phi_k^T P_{\mu_k,\tau_{1(k)},\tau_{2(k)}} \phi_k, \\
&= \mathbb{E}\{(\mathcal{A}\phi(k) + \mathcal{B}_1(\mu(k))\phi(k-\tau_1(k)) + \mathcal{B}_2(\mu(k))\phi(k-\tau_2(k)) \\
&+ \mathcal{B}_3(\mu(k))w(k-\tau_1(k))))^T \bar{P}_{i,m,p}(\mathcal{A}\phi(k) + \mathcal{B}_1(\mu(k))\phi(k-\tau_1(k)) + \mathcal{B}_2(\mu(k))\phi(k-\tau_2(k)), \\
&+ \mathcal{B}_3(\mu(k))w(k-\tau_1(k))))\} - \phi_k^T P_{i,m,p} \phi_k, \\
&= \phi_k^T \mathcal{A}^T \bar{P}_{i,m,p} \mathcal{A}\phi_k + \phi_k^T \mathcal{A}^T \bar{P}_{i,m,p} \mathcal{B}_1^i \phi_{k-\tau_{1(k)}} + \phi_k^T \mathcal{A}^T \bar{P}_{i,m,p} \mathcal{B}_2^i \phi_{k-\tau_{2(k)}} + \phi_k^T \mathcal{A}^T \bar{P}_{i,m,p} \mathcal{B}_3^i w_{k-\tau_{1(k)}}, \\
&+ \phi_{k-\tau_{1(k)}}^T (\mathcal{B}_1^i)^T \bar{P}_{i,m,p} \mathcal{A}\phi_k + \phi_{k-\tau_{1(k)}}^T (\mathcal{B}_1^i)^T \bar{P}_{i,m,p} \mathcal{B}_1^i \phi_{k-\tau_{1(k)}} + \phi_{k-\tau_{1(k)}}^T (\mathcal{B}_1^i)^T \bar{P}_{i,m,p} \mathcal{B}_2^i \phi_{k-\tau_{2(k)}} \\
&+ \phi_{k-\tau_{1(k)}}^T (\mathcal{B}_1^i)^T \bar{P}_{i,m,p} \mathcal{B}_3^i w_{k-\tau_{1(k)}} + \phi_{k-\tau_{2(k)}}^T (\mathcal{B}_2^i)^T \bar{P}_{i,m,p} \mathcal{A}\phi_k + \phi_{k-\tau_{2(k)}}^T (\mathcal{B}_2^i)^T \bar{P}_{i,m,p} \mathcal{B}_1^i \phi_{k-\tau_{1(k)}} \\
&+ \phi_{k-\tau_{2(k)}}^T (\mathcal{B}_2^i)^T \bar{P}_{i,m,p} \mathcal{B}_2^i \phi_{k-\tau_{2(k)}} + \phi_{k-\tau_{2(k)}}^T (\mathcal{B}_2^i)^T \bar{P}_{i,m,p} \mathcal{B}_3^i w_{k-\tau_{1(k)}} + w_{k-\tau_{1(k)}}^T (\mathcal{B}_3^i)^T \bar{P}_{i,m,p} \mathcal{A}\phi_k \\
&+ w_{k-\tau_{1(k)}}^T (\mathcal{B}_3^i)^T \bar{P}_{i,m,p} \mathcal{B}_1^i \phi_{k-\tau_{1(k)}} + w_{k-\tau_{1(k)}}^T (\mathcal{B}_3^i)^T \bar{P}_{i,m,p} \mathcal{B}_2^i \phi_{k-\tau_{2(k)}} + w_{k-\tau_{1(k)}}^T (\mathcal{B}_3^i)^T \bar{P}_{i,m,p} \mathcal{B}_3^i w_{k-\tau_{1(k)}} \\
&- \phi_k^T P_{i,m,p} \phi_k,
\end{aligned} \tag{24}$$

Knowing that,

$$\bar{P}_{i,m,p} = \sum_{j=1}^{4} \sum_{n=0}^{\tau_1^{max}} \sum_{q=0}^{\tau_2^{max}} \Pi_{ij} \Psi_{mn} \Omega_{pq} P_{j,n,q}.$$

$$\mathbb{E}\{\Delta V_2\} = \phi_k^T Q_1 \phi_k - \phi_{k-\tau_1}^T Q_1 \phi_{k-\tau_1} + \phi_k^T Q_2 \phi_k - \phi_{k-\tau_2}^T Q_2 \phi_{k-\tau_2}. \tag{25}$$

$$\mathbb{E}\{\Delta V_3\} = \phi_k^T Q_3 \phi_k - \phi_{k-m}^T Q_3 \phi_{k-m} + \sum_{l=k+1-\tau_{1(k+1)}}^{k-1} \phi_l^T Q_3 \phi_l - \sum_{l=k+1-\tau_{1(k)}}^{k-1} \phi_l^T Q_3 \phi_l$$
$$+ \tau_1 \phi_k^T Q_3 \phi_k - \sum_{l=k+1-\tau_1}^{k} \phi_l^T Q_3 \phi_l + \phi_k^T Q_4 \phi_k - \phi_{k-p}^T Q_4 \phi_{k-p} + \sum_{l=k+1-\tau_{2(k+1)}}^{k-1} \phi_l^T Q_4 \phi_l$$
$$- \sum_{l=k+1-\tau_{2(k)}}^{k-1} \phi_l^T Q_4 \phi_l + \tau_2 \phi_k^T Q_4 \phi_k - \sum_{l=k+1-\tau_2}^{k} \phi_l^T Q_4 \phi_l. \tag{26}$$

It is noticed that,

$$\sum_{l=k+1-\tau_{1(k+1)}}^{k-1} \phi_l^T Q_3 \phi_l + \sum_{l=k+1-\tau_{2(k+1)}}^{k-1} \phi_l^T Q_4 \phi_l = \sum_{l=k+1-\tau_{1(k+1)}}^{k-1} \phi_l^T Q_3 \phi_l + \sum_{l=k+1-\tau_{1(k+1)}}^{k-\tau_{1(k)}} \phi_l^T Q_3 \phi_l$$
$$+ \sum_{l=k+1-\tau_{2(k)}}^{k-1} \phi_l^T Q_4 \phi_l + \sum_{l=k+1-\tau_{2(k+1)}}^{k-\tau_{2(k)}} \phi_l^T Q_4 \phi_l$$
$$\leqslant \sum_{l=k+1-\tau_{1(k)}}^{k-1} \phi_l^T Q_3 \phi_l + \sum_{l=k+1-\tau_1}^{k} \phi_l^T Q_3 \phi_l$$
$$+ \sum_{l=k+1-\tau_{2(k)}}^{k-1} \phi_l^T Q_4 \phi_l + \sum_{l=k+1-\tau_2}^{k} \phi_l^T Q_4 \phi_l, \tag{27}$$

which implies that:

$$\mathbb{E}\{\Delta V_3\} \leqslant \phi_k^T Q_3 \phi_k - \phi_{k-m}^T Q_3 \phi_{k-m} + \tau_1 \phi_k^T Q_3 \phi_k + \phi_k^T Q_4 \phi_k - \phi_{k-p}^T Q_4 \phi_{k-p} + \tau_2 \phi_k^T Q_4 \phi_k. \tag{28}$$

From (24), (25), (28), we can said that:

$$\mathbb{E}\{\Delta V(\phi_k, \mu_k, \tau_{1(k)}), \tau_{2(k)})\} \leq \xi_k^T \Theta_{i,m,p} \xi_k \tag{29}$$

where, $\xi_k = [\phi_k^T \quad \phi_{k-\tau_{1k}}^T \quad \phi_{k-\tau_{2k}}^T \quad \phi_{k-m}^T \quad \phi_{k-p}^T \quad w_{k-\tau_{1k}}^T]^T$.
and,

$$\Theta_{i,m,p} = \begin{bmatrix} \Gamma_{11} & \mathcal{A}^T \bar{P}_{i,m,p} \mathcal{B}_1^i & \mathcal{A}^T \bar{P}_{i,m,p} \mathcal{B}_2^i & 0 & 0 & \mathcal{A}^T \bar{P}_{i,m,p} \mathcal{B}_3 \\ * & \Gamma_{22} & (\mathcal{B}_1^i)^T \bar{P}_{i,m,p} \mathcal{B}_2^i & 0 & 0 & (\mathcal{B}_1^i)^T \bar{P}_{i,m,p} \mathcal{B}_3 + \mathcal{D}_2^i \\ * & * & (\mathcal{B}_2^i)^T \bar{P}_{i,m,p} \mathcal{B}_2^i - Q_2 & 0 & 0 & (\mathcal{B}_2^i)^T \bar{P}_{i,m,p} \mathcal{B}_3 \\ * & * & * & -Q_3 & 0 & 0 \\ * & * & * & * & -Q_4 & 0 \\ * & * & * & * & * & (\mathcal{B}_3)^T \bar{P}_{i,m,p} \mathcal{B}_3 + \mathcal{D}_3^i - \gamma^2 I \end{bmatrix} \tag{30}$$

$\Gamma_{11} = \mathcal{A}^T \bar{P}_{i,m,p} \mathcal{A} - P_{i,m,p} + Q_1 + Q_2 + (1+\tau_1) Q_3 + (1+\tau_2) Q_4$
$\Gamma_{22} = (\mathcal{B}_1^i)^T \bar{P}_{i,m,p} \mathcal{B}_1^i - Q_1 + \mathcal{D}_1^i,$

Using **Lemma** 5.1 (30) becomes as:

$$\begin{bmatrix} -\bar{P}_{i,m,p}^{-1} & \mathcal{A} & \mathcal{B}_1 & \mathcal{B}_2 & 0 & 0 & \mathcal{B}_3 \\ * & \Gamma_{33} & 0 & \cdots & 0 & 0 & 0 \\ * & * & -Q_1+\mathcal{D}_1 & \ddots & 0 & 0 & \mathcal{D}_2 \\ * & * & * & -Q_2 & \ddots & 0 & 0 \\ * & * & * & * & -Q_3 & \ddots & \vdots \\ * & * & * & * & * & -Q_4 & \vdots \\ * & * & * & * & * & * & \mathcal{D}_3-\gamma^2 I \end{bmatrix} < 0, \tag{31}$$

where,

$\Gamma_{33} = -P_{i,m,p} + Q_1 + Q_2 + (1+\tau_1)Q_3 + (1+\tau_2)Q_4$,

We can notice from (31) the existence of non-linear terms. To solve that, we will Pre and Post multiply the matrix by $diag(G_i^T, I, \cdots, I)$ and its transpose [15]. Then, we will use the **Lemma** 5.2. We obtain:

$$\begin{bmatrix} -G^T-G+\bar{P}_{i,m,p} & G^T\mathcal{A} & G^T(\mathcal{B}_1^i) & G^T(\mathcal{B}_2^i) & 0 & 0 & G^T(\mathcal{B}_3^i) \\ * & \Gamma_{33} & 0 & \cdots & 0 & 0 & 0 \\ * & * & -Q_1+\mathcal{D}_1 & \ddots & 0 & 0 & \mathcal{D}_2 \\ * & * & * & -Q_2 & \ddots & 0 & 0 \\ * & * & * & * & -Q_3 & \ddots & \vdots \\ * & * & * & * & * & -Q_4 & \vdots \\ * & * & * & * & * & * & \mathcal{D}_3-\gamma^2 I \end{bmatrix} < 0, \tag{32}$$

where,

$G = \begin{bmatrix} X_1 & 0 \\ 0 & X_2 \end{bmatrix}$.

Lemma 5.3 is used to obtain the LMI in **Theorem** 6.1.

7. Numerical Example

To evaluate the effectiveness of the proposed approach, a numerical example is presented in which a discrete-time linear system is subjected to a sensor fault. In this example, it is assumed that the communication between the sensor and the controller, as well as between the controller and the actuator, occurs over a communication network. Both packet dropout and time delay are considered to exist in both communication links, the simulation data are given as follows :

The system matrices are :

$$A = \begin{bmatrix} 0.1 & 0.3 \\ -1 & 0.8 \end{bmatrix}, \quad B = \begin{bmatrix} 0.39 \\ 0.1 \end{bmatrix}, \quad C = \begin{bmatrix} 1.5 & 0.3 \end{bmatrix},$$
$$E = \begin{bmatrix} 0.2 & 0.2 \end{bmatrix}, \quad F = \begin{bmatrix} 0.1 & 0.1 \end{bmatrix},$$

The sensor noise $d(k) = [W_G(k) \quad 0]^T$ where $W_G(k)$ is a white Gaussian noise with a standard deviation of 0.01, as illustrated in **Figure** 3. The sensor fault signal shown in **Figure** 4, is defined by $f(k) = [f_s(k) \quad 0]^T$ where :

$$f_s(k) = \begin{cases} 1, & 50 \leq k \leq 65, \\ 0, & \text{otherwise.} \end{cases} \tag{33}$$

A square pulse signal was chosen as the fault in order to observe the behaviour of the residual function during the appearance and disappearance of the fault.

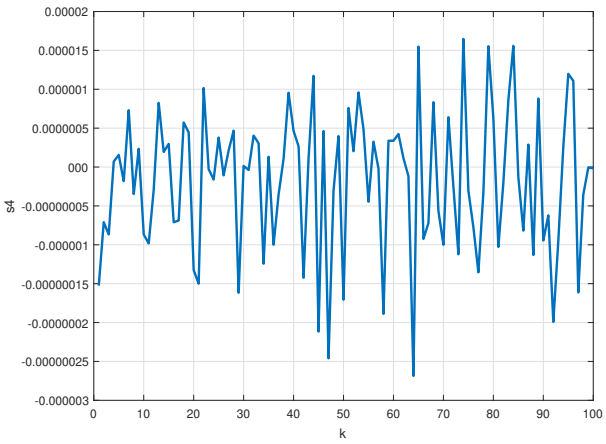


Figure 3: Sensor noise

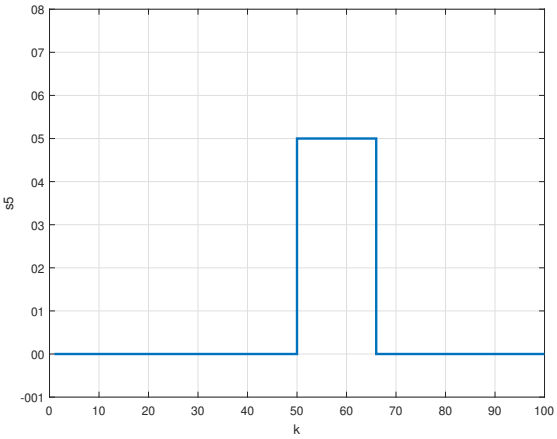


Figure 4: Sensor fault

The switching success rate of both communication links, denoted by S_1 and S_2, is set to 0.9, indicating that 90% of the packets are successfully transmitted through both channels **Figure** 5. The communication delays between the S–C, and between C–A, are modelled as time-varying delays with values $\tau_1 \in \{0, 1\}$ and $\tau_2 \in \{0, 1\}$, respectively, as depicted in **Figure** 6 and **Figure** 7.

The transition probability matrices corresponding to the three Markov chains are given by:

$$\Pi = \begin{bmatrix} 0.01 & 0.04 & 0.05 & 0.9 \\ 0.03 & 0.06 & 0.01 & 0.9 \\ 0.02 & 0.08 & 0 & 0.9 \\ 0 & 0.05 & 0.05 & 0.9 \end{bmatrix}, \quad \Psi = \begin{bmatrix} 0.4 & 0.6 \\ 0.5 & 0.5 \end{bmatrix}, \quad \Omega = \begin{bmatrix} 0.3 & 0.7 \\ 0.6 & 0.4 \end{bmatrix}.$$

The initial conditions are set to $x(k) = [0 \quad 0]^T$ and $\hat{x}(k) = [0.1 \quad -0.1]^T$ for all $k \leq 0$, and the residual gain is defined as $V = 0.1$.

By solving the LMIs presented in the theorem, we obtain the values of the controller and observer gains as follows, $K = [0.3115 \quad 0.2692]$ and $L = [0.0899 \quad 0.1101]^T$. The slack variables are manually selected to ensure a feasible solution. The chosen slack variables are: $\gamma = 0.01$, $\epsilon_1 = 1.33034$, $\epsilon_2 = 1.30281$,$\varpi_1 = 5$ and $\varpi_2 = 3$.

The introduction of slack variables provided more degrees of freedom to the LMI, which helped in finding a feasible solution. Therefore, we can say that our approach remains more

flexible compared to other methods. It is worth highlighting that obtaining a very small value of γ indicates that our approach is highly robust.

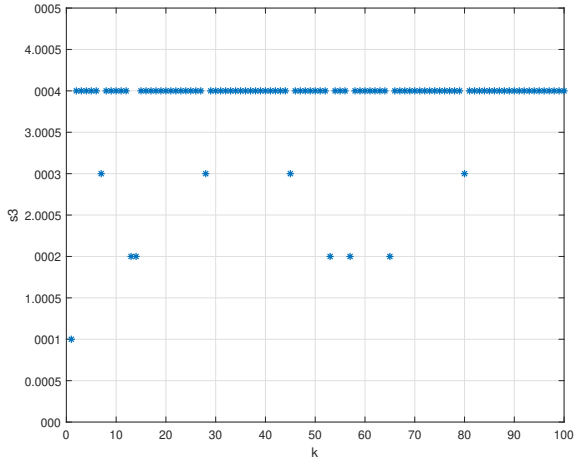


Figure 5: Value of μ_k

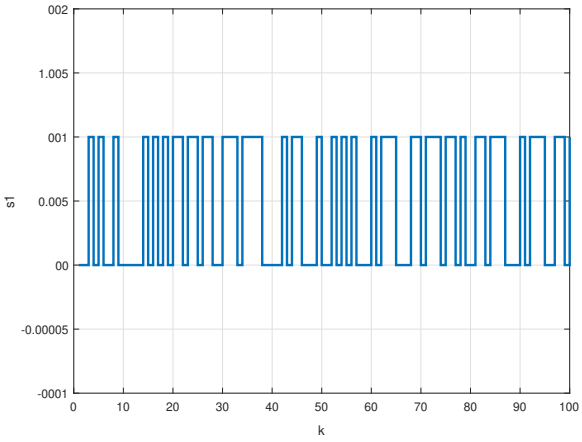


Figure 6: Time delay $\tau_1(k)$.

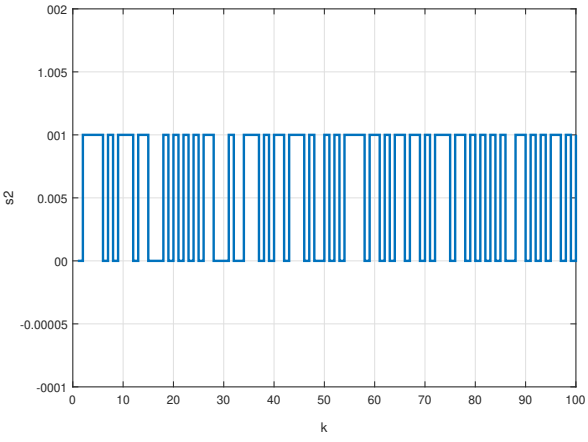


Figure 7: Time delay $\tau_2(k)$.

Figure 8 depicts the behaviour of the residual vector $r(k)$. As shown, the residual exhibits a noticeable change precisely at the fault occurrence time, which is at instant $k = 50$.

Figure 9 shows the evolution of the system state x and the estimated state $\hat{x}$. As illustrated in the figure, we observe that the estimated state converges toward the actual state. A noticeable distortion in both curves can also be observed, especially when the fault occurs at time $k = 50$.

Figure 10 illustrates both the sensor measurement and its corresponding estimation. The impact of the fault on the output signal is clearly noticeable. The estimated signal $\hat{y}(k)$ closely follows and accurately replicates the shape of the actual signal $y(k)$. A slight

delay can be observed between the responses of $y(k)$ and $\hat{y}(k)$ at the moment of fault occurrence, which is attributed to the imperfections in the communication network.

Figure 11 illustrates the residual evaluation function J_k, which provides information about both the occurrence time and the duration of the fault. The detection threshold is set to $J_{\text{th}} = 0.086$ (represented by the blue line), based on a global observation horizon of 100 seconds. The yellow and orange curves represent the system behaviour in the fault-free and faulty scenarios, respectively. As shown, the yellow curve remains below the threshold throughout the simulation, while the orange curve exceeds the threshold at the moment the fault occurs. Specifically, **Figure** 11 shows that $J_{50} = 0.0806 < J_{\text{th}}$ and $J_{51} = 0.1304 > J_{\text{th}}$, Indicating that the fault is detected one step after it occurs, even under the influence of the disturbance input d_k. This highlights the effectiveness of our approach. Rapid and accurate fault detection is crucial for reconfiguring the controller parameters in order to correct or mitigate the fault's impact using a Fault-Tolerant Control (FTC) strategy.

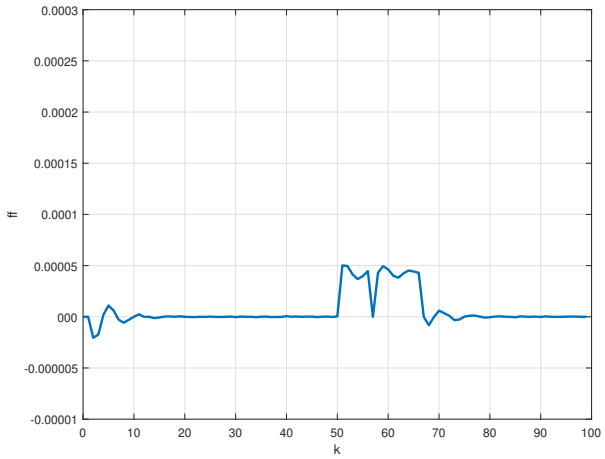


Figure 8: Residual vector.

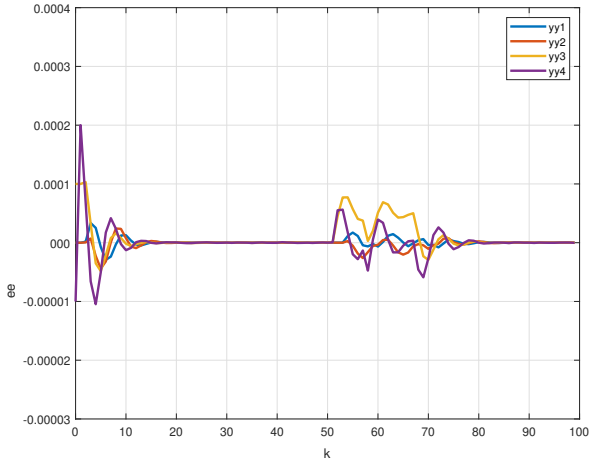


Figure 9: State x and estimate state $\hat{x}$.

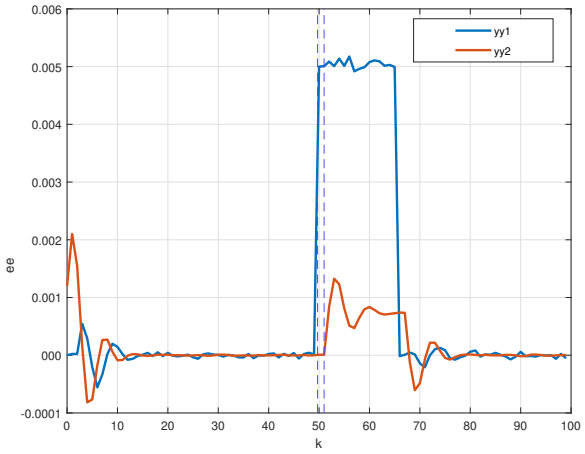


Figure 10: Sensor measurement.

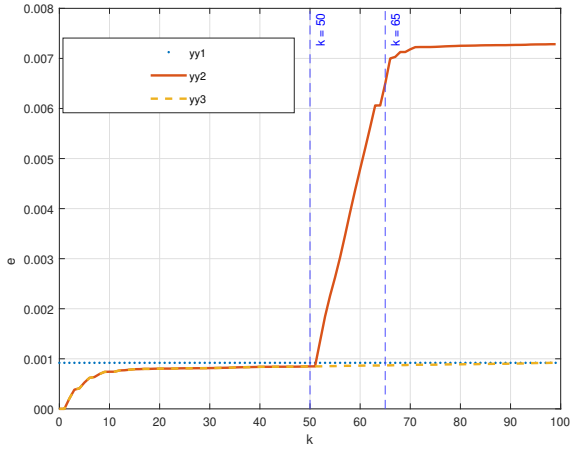


Figure 11: Residual evaluation function J_k and threshold J_{th}.

8. Conclusion

In this work, a robust fault detection strategy was proposed for sensor faults in NCSs affected by communication imperfections, such as packet dropouts and time-varying delays. By modelling the stochastic nature of the network using a Markov chain and incorporating sensor noise, a realistic and comprehensive system representation was achieved. The fault detection problem was formulated within a Lyapunov-based framework, resulting in a set of LMIs that capture both system dynamics and network uncertainties. To improve the feasibility and flexibility of the solution, slack variables were introduced. The proposed method demonstrates the potential for accurate and reliable sensor fault detection, even under adverse communication conditions. The current approach is primarily concerned with fault detection. A promising direction is to enhance the framework to perform fault isolation (identifying which sensor is faulty) and fault estimation (quantifying the fault magnitude).

Competing Interests

The authors declare that they have no competing interests.

Author Contributions

Reda El Abbadi: Conceptualization, Methodology, Investigation, Software, Formal analysis, Writing – Original Draft.
Khalid Badie: Supervision, Validation, Writing – Review & Editing.
Laila Dami: Methodology, Writing – Review & Editing.
Samir Elouaham: Visualization, Validation.
Mohamed Louzazni: Project Administration, Review & Editing.

Funding

The authors received no specific funding for this work.

References

[1] M. S. Mahmoud and M. M. Hamdan, "Fundamental issues in networked control systems," *IEEE/CAA Journal of Automatica Sinica*, vol. 5, no. 5, pp. 902–922, 2018.

[2] X.-M. Zhang, Q.-L. Han, X. Ge, D. Ding, L. Ding, D. Yue, and C. Peng, "Networked control systems: A survey of trends and techniques," *IEEE/CAA Journal of Automatica Sinica*, vol. 7, no. 1, pp. 1–17, 2019.

[3] M. Jaradat, M. Jarrah, A. Bousselham, Y. Jararweh, and M. Al-Ayyoub, "The internet of energy: smart sensor networks and big data management for smart grid," *Procedia Computer Science*, vol. 56, pp. 592–597, 2015.

[4] A. Jabbar, T. Kalsoom, and M. Ur Rehman, "Sensor design for industrial automation," *Multimodal Intelligent Sensing in Modern Applications*, pp. 109–131, 2024.

[5] H. A. Ignatious, M. Khan, *et al.*, "An overview of sensors in autonomous vehicles," *Procedia Computer Science*, vol. 198, pp. 736–741, 2022.

[6] H. Sharma, A. Haque, and F. Blaabjerg, "Machine learning in wireless sensor networks for smart cities: a survey," *Electronics*, vol. 10, no. 9, p. 1012, 2021.

[7] T. M. Ghazal, M. K. Hasan, H. M. Alzoubi, M. Alshurideh, M. Ahmad, and S. S. Akbar, "Internet of things connected wireless sensor networks for smart cities," in *The effect of information technology on business and marketing intelligence systems*, pp. 1953–1968, Springer, 2023.

[8] M. N. Mowla, N. Mowla, A. S. Shah, K. M. Rabie, and T. Shongwe, "Internet of things and wireless sensor networks for smart agriculture applications: A survey," *IEEe Access*, vol. 11, pp. 145813–145852, 2023.

[9] A. Sofi, J. J. Regita, B. Rane, and H. H. Lau, "Structural health monitoring using wireless smart sensor network–an overview," *Mechanical Systems and Signal Processing*, vol. 163, p. 108113, 2022.

[10] R. El Abbadi and H. Jamouli, "Fault detection of a networked control system and its application to a dc motor," *International Journal of Control, Automation and Systems*, vol. 21, no. 6, pp. 1769–1779, 2023.

[11] R. El Abbadi and H. Jamouli, "Stabilization of cyber physical system with data packet dropout and replay attack via switching system approach," in *2019 4th Conference on Control and Fault Tolerant Systems (SysTol)*, pp. 325–329, IEEE, 2019.

[12] R. El Abbadi and H. Jamouli, "Actuator fault estimation of a networked control system with packet loss," *Journal of Control, Automation and Electrical Systems*, vol. 32, pp. 1553–1562, 2021.

[13] S.-Y. Han, Y.-H. Chen, and G.-Y. Tang, "Sensor fault and delay tolerant control for networked control systems subject to external disturbances," *Sensors*, vol. 17, no. 4, p. 700, 2017.

[14] Y.-Y. Zhang, J.-L. Zhang, X.-Y. Luo, and X.-P. Guan, "Sensor/actuator faults detection for networked control systems via predictive control," *International Journal of Automation and Computing*, vol. 10, no. 3, pp. 173–180, 2013.

[15] A. Benzaouia and K. Telbissi, "Actuator fault estimation based on proportional integral observer for discrete-time switched systems," *Journal of Dynamic Systems, Measurement, and Control*, vol. 141, no. 3, 2019.

[16] R. El Abbadi and H. Jamouli, "Stabilization of cyber physical system exposed to a random replay attack modeled by markov chains," in *2019 6th International Conference on Control, Decision and Information Technologies (CoDIT)*, pp. 528–533, IEEE, 2019.

[17] R. El Abbadi and H. Jamouli, "Takagi–sugeno fuzzy control for a nonlinear networked system exposed to a replay attack," *Mathematical Problems in Engineering*, vol. 2021, 2021.

[18] L. Qiu, Q. Luo, F. Gong, S. Li, and B. Xu, "Stability and stabilization of networked control systems with random time delays and packet dropouts," *Journal of the Franklin Institute*, vol. 350, no. 7, pp. 1886–1907, 2013.

[19] Z. Wang, D. W. Ho, and X. Liu, "Variance-constrained filtering for uncertain stochastic systems with missing measurements," *IEEE Transactions on Automatic control*, vol. 48, no. 7, pp. 1254–1258, 2003.

[20] F. Zhang, *The Schur complement and its applications*, vol. 4. Springer Science & Business Media, 2006.

[21] A. Benzaouia, M. Ouladsine, A. Naamane, and B. Ananou, "Fault detection for uncertain delayed switching discrete-time systems," *International Journal of Innovative Computing, Information and Control*, vol. 8, no. 12, pp. 8049–8062, 2012.